Institute of Paper Science and Technology
Atlanta, Georgia

IPST Technical Paper Series Number 639

Flash X-Ray Radiography for Visualizing Gas Flows in Opaque Liquid/Fiber Suspensions

T.J. Heindel and J.L. Monefeldt

February 1997

Submitted to
6th International Symposium on Gas-Liquid Two-Phase Flows
ASME Fluids Engineering Division Summer Meeting
Vancouver, British Columbia, Canada
June 22–26, 1997

INSTITUTE OF PAPER SCIENCE AND TECHNOLOGY
PURPOSE AND MISSIONS

The Institute of Paper Science and Technology is a unique organization whose charitable, educational, and scientific purpose evolves from the singular relationship between the Institute and the pulp and paper industry which has existed since 1929. The purpose of the Institute is fulfilled through three missions, which are:

- to provide high quality students with a multidisciplinary graduate educational experience which is of the highest standard of excellence recognized by the national academic community and which enables them to perform to their maximum potential in a society with a technological base; and
- to sustain an international position of leadership in dynamic scientific research which is participated in by both students and faculty and which is focused on areas of significance to the pulp and paper industry; and
- to contribute to the economic and technical well-being of the nation through innovative educational, informational, and technical services.

ACCREDITATION

The Institute of Paper Science and Technology is accredited by the Commission on Colleges of the Southern Association of Colleges and Schools to award the Master of Science and Doctor of Philosophy degrees.

FLASH X-RAY RADIOGRAPHY FOR VISUALIZING GAS FLOWS IN OPAQUE LIQUID/FIBER SUSPENSIONS

Theodore J. Heindel and James L. Monefeldt[1]
Engineering and Paper Materials Division
Institute of Paper Science and Technology
Atlanta, Georgia 30318-5794
ted.heindel@ipst.edu

ABSTRACT

Gas flows in opaque suspensions are important to many process industries, but understanding the behavior of such flows is complicated by limited visual access. Additional difficulties arise when a component of the opaque suspension is fibrous, which could form entanglements around any instrument or sampling probe inserted into the suspension. These types of gas/liquid/fiber suspensions are very important to the pulp and paper industry because they are found throughout the many paper processing steps, including flotation deinking and bleaching.

This paper will discuss the use of flash x-ray radiography (FXR) to visualize air flows in an air/water/wood fiber suspension. Air has a different x-ray attenuation coefficient compared to water, while wood fiber and water have similar attenuation coefficients. Therefore, FXR provides stop-motion images of air bubbles rising through an opaque fibrous pulp suspension. FXR flow visualization will be described, and images comparing air/water flows to air/water/wood fiber flows will be presented for various air flow rates and wood fiber consistencies (percent of fiber by weight).

The fundamental flow pattern differences observed when wood fibers are added to an air/water system will also be highlighted. Specifically, discrete air bubbles in an air/water/fiber system remain spherical at relatively large sizes when compared to an air/water system at similar air flow rates, and discrete channels are formed in the fiber suspension, which create preferential rise paths for air bubbles. Additionally, the presence of fibers enhances bubble coalescence and induces churn-turbulent flow conditions at relatively low air flow rates.

INTRODUCTION

A greater understanding of the fluid dynamic behavior of complex multiphase systems is important to many industries, including mineral processing, oil recovery, and paper manufacturing. Insight into the system behavior can be gained by optical visualization techniques if the system is transparent, typical of many air/water systems. Information such as flow regime, bubble size, and bubble velocity may be gathered. When the system is translucent or opaque, common in many multiphase systems, such information may be obtained by inserting selected probes into the system to measure parameters of interest. Measurement and visualization techniques for many multiphase systems have been described in monographs by Clift et al. (1978), Hetsroni (1982), and Shook and Roco (1991). Additional review articles have also appeared (e.g., Saxena et al., 1988).

Complex multiphase systems that are translucent or opaque and have one phase that may interact with, or impede the performance of, intrusive probes cannot be investigated with traditional experimental tools like high-speed video, electrical resistivity probes, or optical probes. One such system involves air, water, and wood fibers common to wastepaper processing. In particular, flotation deinking utilizes air bubbles to remove hydrophobic particles between approximately 20 to 200 μm in diameter from wastepaper slurries composed of water, fiber, and other contaminant particles (McCool, 1993; Ferguson, 1995). Air bubbles are introduced into the system where the hydrophobic particles attach to the hydrophobic bubble surface. As the bubbles rise, they carry the contaminants to the surface where they are skimmed, leaving clean fiber behind to be used as recycled material. Bubble behavior in this system is very important because it has a direct effect on the contaminant removal efficiency. For example, a bubble must be large enough to produce a sufficient buoyant force to rise through the fiber network. However, if the bubble is too large, overall bubble surface area will be significantly reduced for a given total air volume, which reduces the area contaminant particles can attach

[1] Current address: Champion International Corporation
Courtland, Alabama

to. Additionally, large bubbles may reduce flotation efficiency by promoting the formation of discrete regions in the suspension where the majority of the air rises (defined as channeling), leaving some regions deficient of air bubbles. A second process common in paper processing comprising gas, water, and fiber involves gaseous fiber bleaching where, for example, ozone is introduced into a 1-3% consistency wood pulp suspension (Lindholm, 1986). The ozone carrier gas must be well mixed with the wood fibers to ensure uniform bleaching reactions. Ideally, a homogeneous system would provide more efficient flotation and bleaching than a heterogeneous system. However, a systematic flow regime study has yet to be performed due to the complexities of this system.

Attempts to visualize these complex fiber suspensions have been conducted by Walmsley (1992) where water was replaced by clove oil to produce a system that had the same refractive index as wood fiber. However, the applicability of these results to air/water/fiber systems is unknown. Additional experiments have been performed to measure bubble size in dilute fiber systems less than 0.5% consistency by weight (Göttsching et al., 1995), but extension to higher consistency systems has yet to be published. Therefore, additional tools and/or techniques must be developed. One such technique that can be used to visualize complex multiphase systems is flash x-ray radiography.

FLASH X-RAY RADIOGRAPHY

Flash x-ray radiography (FXR) is an x-ray process where an intense burst of radiation is produced for a fraction of a second to record dynamic events on film that may be obscured by dust, smoke, or light that would make conventional photography impossible. FXR also allows for images to be recorded of inclusions or voids inside opaque objects that are part of these dynamic events. Current areas where FXR is commonly utilized include high velocity ballistics, explosives, weapons development, nondestructive testing, and medical and biological studies (Physics International, 1996).

The fundamentals of FXR are similar to traditional x-ray radiography (Jamet and Thomer, 1976; Cartz, 1995; Physics International, 1996). A radiograph is a photographic record of an object produced on film exposed by the penetration and scattering of x-rays through the object. Therefore, a radiograph is a shadow picture of an object with lighter images associated with object areas of greatest density. The ratio of the dimensions of the object and image is the same as the ratio of the distances between the source and object and the source and film. Hence, ideal radiographic conditions include: (1) minimize the radiation source size, (2) maximize the source to object distance, (3) minimize the object to film distance, (4) incident radiation should be perpendicular to the plane of the object, and (5) the plane of the object should be parallel to the film (Cartz, 1995).

X-ray image quality is dependent on the contrast developed in the radiograph due to the x-ray attenuation characteristics of the materials in the system of interest. Contrast may be reduced by several independent mechanisms, some due to x-ray absorption, others due to x-ray scattering. Contrast may be enhanced by film selection, the use of intensifying screens, or by filtering the x-ray beam with a thin metal screen. However, optimal contrast is not easy to obtain, and each object/film/screen/filter combination must be analyzed by trial and error to determine the best sharpness, clarity, contrast, and resolution. Detailed descriptions of x-ray techniques can be found in any text describing radiography (e.g., Jamet and Thomer, 1976; Cartz, 1995).

FXR has the ability to penetrate fluids that are opaque and produce a permanent film record of high-speed events. Impact visualization is a recent example of visualizing high-speed events (Grady and Kipp, 1994). FXR has also been used to visualize boiling in metal tubes under high pressures (Bennett et al., 1965). Nontraditional uses of FXR include paper sheet forming (Farrington, 1986), spray formation (Farrington, 1988), coating applications (Triantafillopoulos and Farrington, 1988), and impulse drying (Zavaglia and Lindsay, 1989). The commonality between these processes is that the event of interest is high speed and the region of visual interest is obscured – ideal for application to FXR.

The application of FXR to air/water/fiber flows is justified because water and wood fibers have similar densities, whereas the density of air is considerably different from water and wood fiber. Water also has a linear x-ray attenuation coefficient three orders of magnitude larger than air, and a dilute suspension of wood fiber and water should absorb x-rays in a similar manner, unless the water or fiber has been treated with special radioactive materials. Therefore, the water and wood fibers will absorb x-rays at a different rate compared to air. In this study, FXR will be used to visualize air flows in a fibrous pulp suspension at various fiber consistencies and air flow rates to compare and contrast these flows to air/water systems.

EXPERIMENTAL METHODS

Figure 1 is a schematic representation of the experimental setup used in this study. The entire system is housed in a 3.5 m × 4.5 m room lined with lead foil for safety considerations. A planar bubble column, with interior dimensions 20 cm wide by 2 cm deep, was constructed with face panes of 6.35 mm clear acrylic stock. The column was 1 m tall with lead numbers affixed to both sides to indicate the column height, which was recorded on film when x-rays were taken. A planar bubble column was chosen to provide a uniform x-ray penetration across the width of the column when filled with a homogeneous fluid. This results in a uniform exposure density on the x-ray film if no bubbles are present. FXR could also be used to visualize flows in cylindrical columns.

Compressed air was injected into the base of the column through nine evenly spaced holes along the central axis of a 3.18 mm thick n-butyl rubber gasket. The holes were formed in the gasket with a 0.34 mm diameter drill bit and were self-sealing when the air pressure was removed. The rubber gasket separated the bubble column from a conical air diffuser and allowed for the possibility of using different air injection patterns and/or hole sizes. Air flow was regulated with a Dixon air regulator and filter, and was measured with one of two Sierra Instruments mass flow meters, one covering air flow rates less than 1 slpm (standard liter per minute) and one covering air flow rates less than 40 slpm. The entire bubble column was

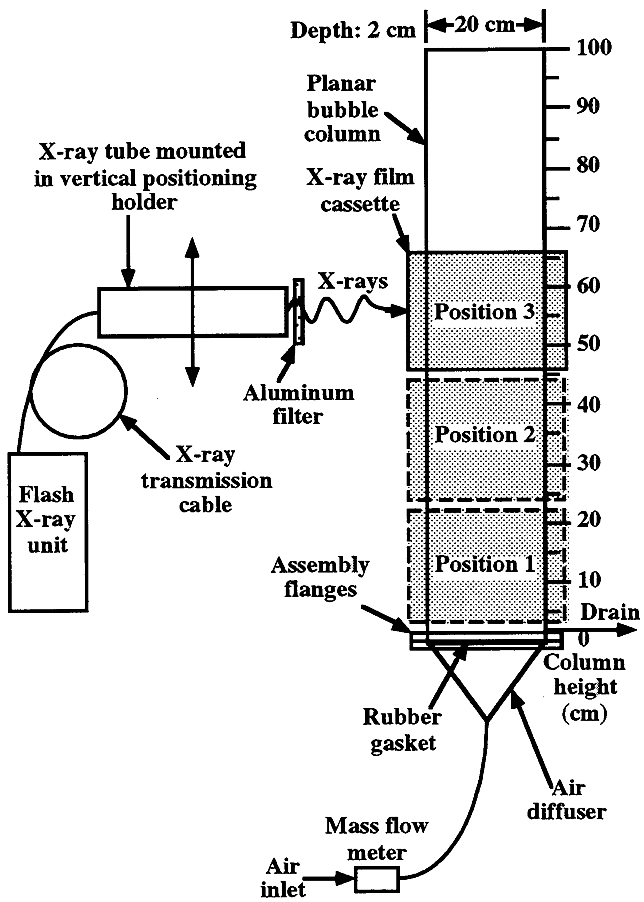

FIGURE 1: EXPERIMENTAL SETUP.

mounted on a support stand with locking wheels to allow horizontal placement from the x-ray source.

The x-ray unit used in this study was a 300 keV HP 43733A flash x-ray system (currently supported by Physics International), which generates a 30 nanosecond x-ray pulse. The x-ray tube head was mounted in a locking vertical slide to allow x-ray exposures at various heights. Since this system produces a range of x-ray energies, a 3.25 mm aluminum filter was mounted directly in front of the x-ray window to filter soft x-rays (long wavelength, low energy x-rays) that promote scattering effects and result in fuzzy images (Cartz, 1995). The resulting hardened x-ray beam (short wavelength, high energy x-rays) produced sharper images with improved contrast.

A single 20 cm × 25.2 cm x-ray negative was exposed during the discharge of the x-ray unit. The x-ray film was either AGFA D8 or D6 Structurix film and was mounted in a film cassette between two Dupont Quanta Rapid Back PF intensifying screens. This was performed in a lightproof room where the x-ray negatives were also developed manually (film developing details can be found in Monefeldt, 1996). Each film cassette was attached to the back of the bubble column in the orientation and in one of three positions identified in Fig. 1. A lead letter/number identification was also taped to each cassette to permanently identify the image when developed. The x-ray source was located in front of, and perpendicular to, the planar bubble column. All radiographs were taken at a source to film distance of 1.65 m and an object to film distance of 1.6 cm. The bubble column and x-ray tube were aligned using a laser pointer mounted to the top of the x-ray tube such that the x-ray source was coincident with the center of the x-ray film.

The air/water system used in this study consisted of compressed and filtered building air and deionized water. Air/water/fiber systems were composed of deionized water and unprinted old newsprint (wood pulp fibers). The old newsprint was reslushed following TAPPI method T 205 om-88 (TAPPI, 1994), however, deionized water was used, and the disintegration was performed at 1.5% consistency (percent of dry fiber by weight). Three samples from this slurry were analyzed with a Kajaani FS-100 fiber length analyzer for fiber length characterization, yielding a weighted mean fiber length of 1.3 mm. Pulp slurries of 0.5% and 1.0% consistency were prepared by diluting samples of the 1.5% consistency stock with deionized water. Formaldehyde (37% solution) was added to the samples (2.0 cm^3/l) to prevent biological degradation. It was assumed that this small amount of formaldehyde did not significantly affect the flow characteristics.

The system was charged by filling the column from the top to a fluid height of 80 cm. This allowed for fluid expansion in the column once air was introduced into the system. The column was drained when not in use through a valved opening located on the column side near its base. After filling, wood fiber suspensions slowly separate over a period of hours and local high consistency regions may form if the system is not agitated. Therefore, a high air flow rate was maintained to keep the system well mixed and inhibit fiber network formation, which is common at high consistencies. After an experiment was set up and the x-ray film was properly placed, the air flow rate was adjusted to the desired level. A waiting period of 10-15 minutes allowed the flow to reach steady-state conditions, whereupon an x-ray was taken. A total of 176 x-ray images were obtained in this study.

Verification of the FXR technique to capture a true image of air bubbles rising through water was completed by Monefeldt (1996) by comparing images acquired with high-speed video photography with those obtained at the same time (± 0.033 sec) using FXR. Very good qualitative agreement was obtained and identical bubbles and bubble groups were identified on both the video and FXR images, indicating that this FXR does record air bubbles rising through a liquid medium.

RESULTS

Flash x-rays of an air/water system and an air/water/fiber system at 0.5%, 1.0%, and 1.5% consistency were obtained at three locations in a planar bubble column over a range of volumetric air flow rates (V) of 0.25 slpm $\leq V \leq$ 30 slpm. This corresponds to a superficial gas velocity of 0.10 cm/s $\leq u_g \leq$ 12.5 cm/s, where $u_g = V/A_c$ with A_c representing the column cross-sectional area. From a comparison of the 176 x-ray images, three flow regimes are identified: (1) bubbly flow indicates small, dispersed bubbles are rising throughout the column width in a homogeneous pattern; (2) churn-turbulent flow implies large bubbles formed by the coalescence of smaller bubbles are found throughout the column width, with the possibility of some small bubbles still present, but the flow is fairly heterogeneous; and (3) transitional flow denotes the transition from bubbly to churn-turbulent flow and is identified by dispersed small bubbles throughout the column width and some larger bubbles due to coalescence, but not observed throughout the column width. Slug flow is not observed because the column used in this study was too wide. As described by Hewitt (1982), wide-bore tubes promote oscillatory motion which prevents slug formation.

X-rays of an Air/Water System

Figure 2 displays x-rays obtained in an air/water system at three different column heights with an air flow rate of V = 1 slpm (u_g = 0.42 cm/s). Each image was taken at a separate time interval, and this figure represents a composite of the conditions at each column position. The gap between the channel bottom where the air is introduced and the beginning of the first image is due to the flange and bolts that are used to attach the column to the diffuser preventing the film cassette from being placed any lower. The gaps between Positions 1 and 2 and Positions 2 and 3 are caused by the film cassette holder being fixed at specific column locations. The actual image that encompassed the column was 20 cm × 20 cm with approximately 2.5 cm of film overhanging each side, which included the lead position indicators and radiograph identification label. The radiograph portions including the identification and location numbers have been removed from the images presented here to increase clarity. The reproduced and reduced images do have some loss of detail, but the images are representative of the originals, which are available at the Institute of Paper Science and Technology. All observations are based on the original images.

At V = 1 slpm, the images from Positions 1 to 3 do not vary significantly, and a bubbly flow regime throughout the column is observed with elliptical-shaped bubbles evenly dispersed across the column width. Increasing the air flow rate increased the number of rising bubbles, while the bubble shape and size remained approximately uniform until bubbles began to coalesce. This occurred at V ≈ 2.5 slpm (u_g ≈ 1.0 cm/s), indicating the beginning of the transition to churn-turbulent flow (i.e., transitional flow). Increasing the air flow rate further increased the bubble coalescence rate, and churn-turbulent flow is observed at Position 3 when V ≈ 4.0 slpm (u_g ≈ 1.7 cm/s). Churn-turbulent flow is observed throughout the column when V ≈ 7.5 slpm (u_g ≈ 3.1 cm/s). The observation of churn-turbulent flow at Position 3 at lower flow rates than at Position 1 is expected because bubbles have a chance to coalesce as they rise through the column.

An example of radiographs of churn-turbulent flow in the entire column is shown in Fig. 3 for V = 10 slpm (u_g = 4.2 cm/s). The large dark regions are single bubbles resulting from the coalescence of many smaller bubbles. Some are formed at the column base as the air is introduced into the column at such high flow rates. Others form as the bubbles rise through the column and they interact with each other in this highly turbulent flow.

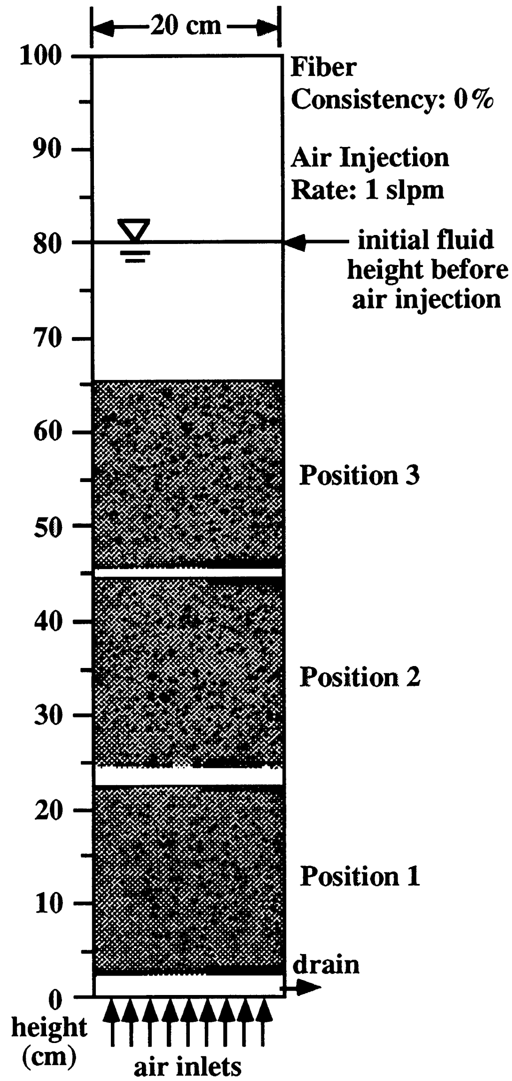

FIGURE 2: RADIOGRAPHS OF AN AIR/WATER SYSTEM AT V = 1 slpm (u_g = 0.42 cm/s).

At these high air flow rates, backmixing is visually observed in the column, where large bubbles (that may span the column depth) travel up the column in a serpentine pattern and smaller bubbles travel downward, trapped in the backmixed flow around the oscillating rising channels of air. The smaller bubbles are eventually caught in the rising bulk flow. Backmixing is not captured on the x-ray images.

X-rays of an Air/Water/Fiber System at 1% Consistency

Differences between the observed flow in an air/water system and one including fibrous material are demonstrated at a wood fiber consistency of 1%. Figure 4 displays radiographs obtained at the three column positions for an air flow rate of V = 1 slpm (u_g = 0.42 cm/s) with 1% by weight wood fiber added to the air/water system. This figure can be directly compared to

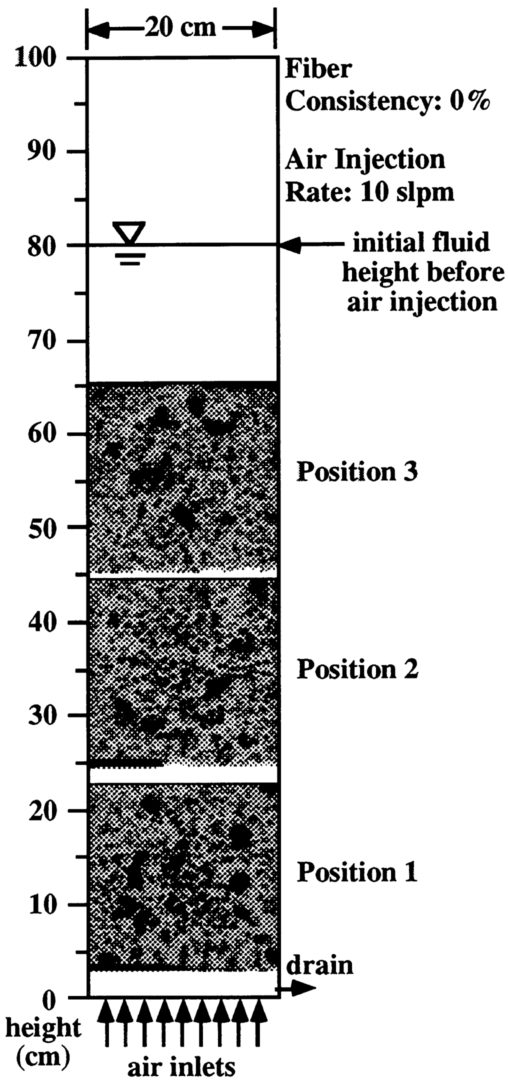

FIGURE 3: RADIOGRAPHS OF AN AIR/WATER SYSTEM AT V = 10 slpm (u_g = 4.2 cm/s).

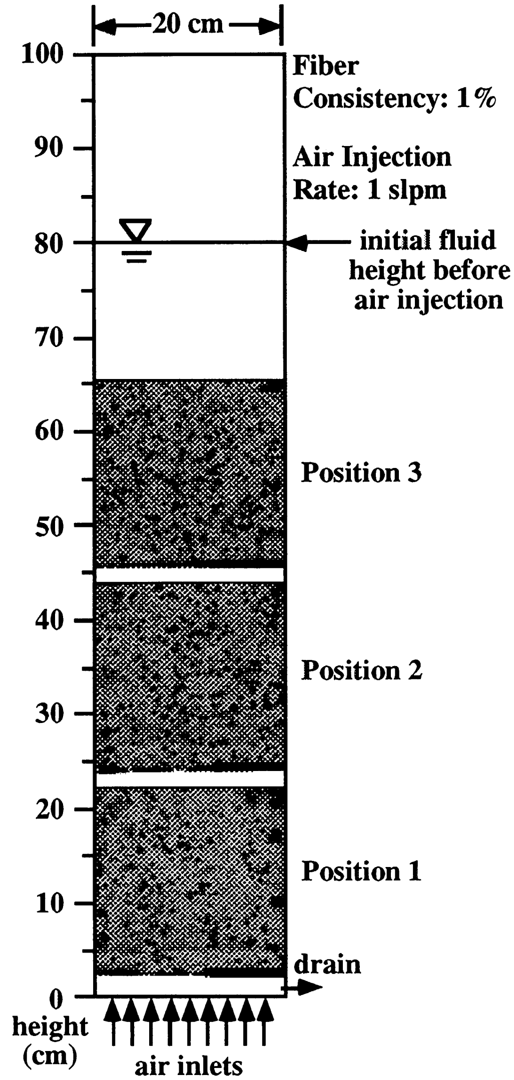

FIGURE 4: RADIOGRAPHS OF AN AIR/WATER/FIBER SYSTEM AT V = 1 slpm (u_g = 0.42 cm/s).

the air/water system shown in Fig. 2. With 1% consistency of wood fiber, small spherical bubbles are dispersed throughout the channel and larger bubbles are observed at some locations. The larger bubbles are hypothesized to be due to bubble coalescence promoted by the introduction of fibers. Hence, Fig. 4 displays the beginning of the transitional flow regime between bubbly and churn-turbulent flow. The larger bubbles rise faster in the system due to the increased buoyant force. This creates channels in the air/water/fiber system where the local mass concentration of fiber is reduced, which provides a preferential, low resistance flow path for the rising air and promotes additional bubble coalescence. This phenomenon was also observed by Walmsley (1992) in an air/clove oil/fiber system. Channeling can be a disadvantage to any fibrous system where a gas is injected because efficient system operation is typically associated with a homogeneous gas dispersion. When channeling occurs, regions within the fiber suspension may be completely void of gas, producing a heterogeneous suspension, which is detrimental in the paper industry, particularly with flotation deinking and ozone bleaching (Lindholm, 1986).

For the 1% consistency fibrous system in this study, bubbly flow was observed throughout the channel when $V \lesssim 1.0$ slpm ($u_g \lesssim 0.42$ cm/s), and churn-turbulent flow was observed at all three positions when $V \gtrsim 3.1$ slpm ($u_g \gtrsim 1.3$ cm/s). Only small differences in the transition regions were observed at the three column positions for the 1% consistency system, implying fibers promote flow regimes that are more uniform throughout the column height.

At high air flow rates, such as V = 10 slpm (u_g = 4.2 cm/s), very large bubbles are visually observed that span the entire column depth of 2 cm and rise in a central oscillating channel. This is captured on x-ray film as very large bubbles in

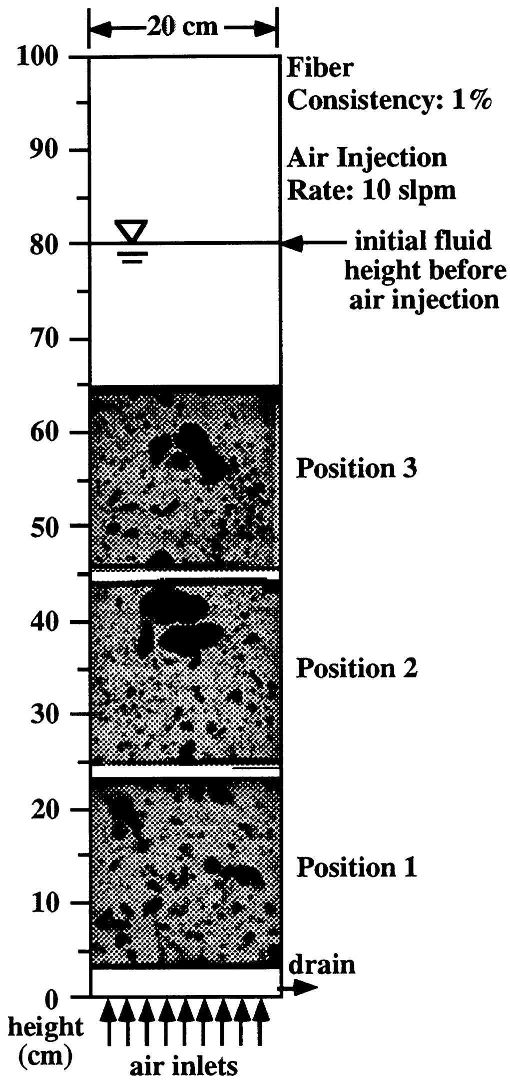

FIGURE 5: RADIOGRAPHS OF AN AIR/WATER/FIBER SYSTEM AT V = 10 slpm (u_g = 4.2 cm/s).

one area of the channel, with other bubbles that are not quite as large elsewhere, as shown in Fig. 5. The many large bubbles in Position 1 coalesce to form even larger bubbles that rise in an oscillatory pattern in Positions 2, 3, and toward the fluid surface. The oscillations cause backmixing, which is not specifically captured on the radiographs. Selected x-rays also showed large groupings of smaller bubbles or small bubbles following in the wake of larger bubbles. It is hypothesized that these groupings are in the process of coalescing, but frozen in time due to the flash x-ray image recording process.

Comparing Figs. 3 and 5, which are for the same flow conditions, the presence of fibers at the high air flow rates results in very large bubbles and fewer small bubbles. The fibers enhance coalescence and promote heterogeneous flow.

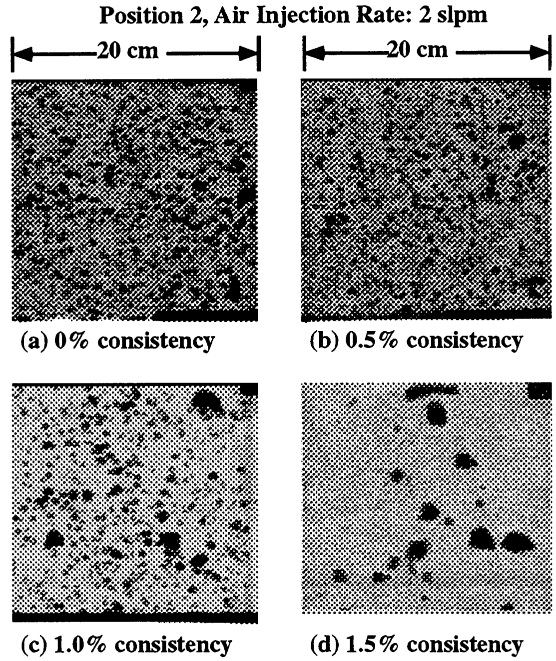

FIGURE 6: EFFECT OF FIBER CONSISTENCY AT V = 2 slpm (u_g = 0.83 cm/s).

Effect of Fiber Consistency

The effect of fiber consistency on the flow patterns is determined by comparing radiographs taken at fiber consistencies of 0% (the air/water system), 0.5%, 1.0%, and 1.5%. This range of consistencies is very important for the wastepaper processing industry because flotation deinking is typically carried out at consistencies between 0.8% and 1.2% (Ferguson, 1995).

Qualitative comparisons of the x-rays from the various systems reveal that adding wood fibers to an air/water system results in bubbles that are slightly larger, more spherical, and less numerous when the air injection rate is constant. Observations indicate that the smallest bubbles generated in the 1.5% wood fiber slurry were larger than the smallest bubbles produced in the other systems. This is due to the formation of a fiber network (flocculation) at this consistency. A larger buoyant force (i.e., bubble size) is required to break through this fiber network. This phenomenon was primarily observed in the 1.5% consistency system.

As shown in Fig. 6 for Position 2 and V = 2 slpm (u_g = 0.83 cm/s), increasing the fiber consistency from 0% to 1.5% results in fewer, but larger bubbles recorded on the radiographs because the fibers enhance bubble coalescence. This is most significant for the given conditions at consistencies between 1.0% and 1.5%. The fewer, larger bubbles result in a significant reduction in the overall bubble surface area, which will be detrimental to any process where maximizing gas bubble surface area is important.

By identifying the flow regime of each of the 176 radiographs, a flow regime map can be constructed for the various flow rates and consistencies addressed in this study. As

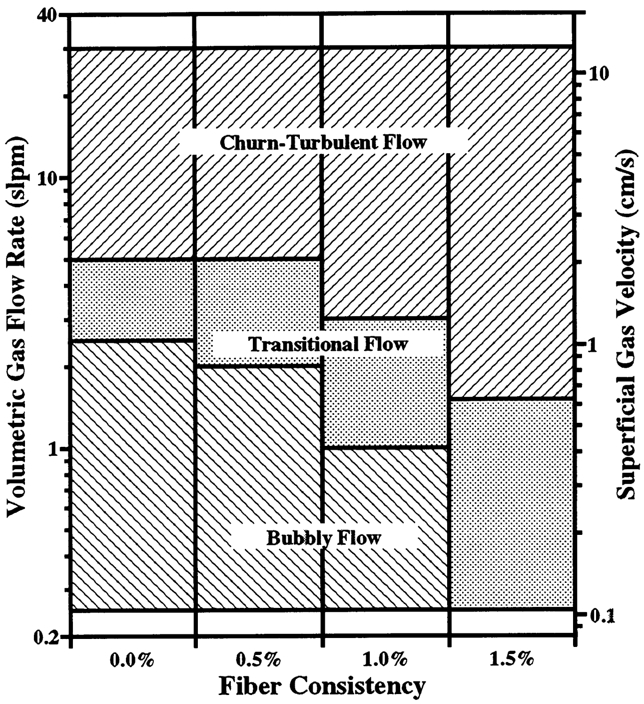

FIGURE 7: FLOW REGIME MAP OF THE PLANAR BUBBLE COLUMN AT POSITION 2.

shown in Fig. 7 for Position 2, increasing the fiber consistency results in transitional and churn-turbulent flow at lower air flow rates. At a consistency of 1.5%, bubbly flow is not observed even at the lowest air flow rate considered in this study (V = 0.25 slpm; u_g = 0.10 cm/s). Under these conditions, channels form as soon as air is introduced into the system and coalesces with other bubbles to form air bubbles large enough to rise through the fiber network. This implies that any process requiring a homogeneous gas mixture in a fiber network would also require some form of assisted mixing, even when fiber consistencies are as low as 1.5%.

Similar results are observed with other channel positions identified in this study. Minor differences occur between positions for some consistencies, where transitional and churn-turbulent flow may be delayed to slightly higher air flow rates at Position 1, but hastened to slightly lower air flow rates at Position 3. This results from bubbles coalescing as they rise from Position 1 to Position 3. However, these variations are small, and Fig. 7 is a good representation of the flow regimes observed in this study.

CONCLUSIONS

Flash x-ray radiography (FXR) was utilized to visualize the flow behavior of an air/water system and an air/water/fiber system in a planar bubble column over a range of air flow rates and fiber consistencies. FXR was shown to be an effective technique to visualize dynamic fiber systems at discrete instants in time. In general, the presence of fibers produced bubbles that were more spherical and promoted coalescence when compared to a simple system of air and water. The transition from bubbly to churn-turbulent flow also occurred at lower air flow rates as the fiber consistency increased.

ACKNOWLEDGMENTS

Financial support of this work by the Institute of Paper Science and Technology and its Member Companies is gratefully acknowledged. Portions of this work were used by James Monefeldt in partial fulfillment of the requirements for the M.S. degree at the Institute of Paper Science and Technology. Special thanks is extended to Paul Phelan for FXR training and troubleshooting. Additionally, the help of Adele Emery with digitizing the radiographs for presentation purposes is gratefully acknowledged.

REFERENCES

Bennett, A. W., Hewitt, G. F., Kearsey, H. A., Keeys, R. K. F., and Lacey, P. M. C., 1965, "Flow Visualization Studies of Boiling at High Pressure," *Proceedings of the Institution of Mechanical Engineers, Part 3C*, Vol. 180, pp. 1-11.

Cartz, L., 1995, *Nondestructive Testing*, ASM International, Materials Park, OH.

Clift, R., Grace, J. R., and Weber, M. E., 1978, *Bubble, Drops, and Particles*, Academic Press, New York.

Farrington, T. E., Jr., 1986, "A More Fundamental Approach to the Problem of High Consistency Forming," *1986 TAPPI Engineering Conference*, Atlanta, GA, TAPPI, pp. 709-717.

Farrington, T. E., Jr., 1988, "Flash X-ray Imaging of Kraft Black Liquor Sprays," *TAPPI Journal*, Vol. 71, pp. 89-92.

Ferguson, L. D., 1995, "Flotation Deinking Technology," *1995 Deinking Short Course*, Vancouver, WA, TAPPI Press, Chapter 10.

Göttsching, L., Hunold, M., Krauthauf, T., Müller, J., and Putz, H.-J., 1995, "Effect of Air Volume and Air Bubble Size Distribution on Flotation in Injector Aerated Deinking Cells," *3rd Research Forum on Recycling*, Vancouver, BC, pp. 17-25.

Grady, D. E., and Kipp, M. E., 1994, "Experimental and Computational Simulation of the High Velocity Impact of Copper Spheres on Steel Plates," *International Journal of Impact Engineering*, Vol. 15, pp. 645-660.

Hetsroni, G., Ed., 1982, *Handbook of Multiphase Systems*, Hemisphere Publishing Corp., New York.

Hewitt, G. F., 1982, "Flow Regimes," *Handbook of Multiphase Systems*, G. Hetsroni, Ed., Hemisphere Publishing Corp., New York, Chapter 2.1.

Jamet, F., and Thomer, G., 1976, *Flash Radiography*, Elsevier Publishing Company, Inc., New York.

Lindholm, C.-A., 1986, "Effect of Heterogeneity in Pulp Bleaching with Ozone," *Paperi ja Puu*, Vol. 68, pp. 283-290.

McCool, M. A., 1993, "Flotation Deinking," *Secondary Fiber Recycling*, R. J. Spangenberg, Ed., TAPPI Press, Atlanta, pp. 141-162.

Monefeldt, J. L., 1996, Flow Structures in a Quiescent Rectangular Bubble Column, M.S. Thesis, Institute of Paper Science and Technology, Atlanta, GA.

Physics International, 1996, Flash X-ray Seminar, San Leandro, CA.

Saxena, S. C., Patel, D., Smith, D. N., and Ruether, J. A., 1988, "An Assessment of Experimental Techniques for the Measurement of Bubble Size in a Bubble Slurry Reactor as Applied to Indirect Coal Liquefaction," *Chemical Engineering Communications*, Vol. 63, pp. 87-127.

Shook, C. A., and Roco, M. C., 1991, *Slurry Flow: Principles and Practice*, Butterworth-Heinemann, Boston.

TAPPI, 1994, "T 205 om-88 - Forming Handsheets for Physical Tests of Pulp," TAPPI Test Methods 1994-1995, TAPPI Press, Atlanta.

Triantafillopoulos, N. G., and Farrington, T. E., Jr., 1988, "Flash X-ray Radiography Techniques for Visualizing Coating Flows," *1988 TAPPI Coating Conference*, New Orleans, LA, TAPPI, pp. 47-52.

Walmsley, M. R. W., 1992, "Air Bubble Motion in Wood Pulp Fibre Suspension," *APPITA 1992 Proceedings*, pp. 509-515.

Zavaglia, J. C., and Lindsay, J. D., 1989, "Flash X-Ray Visualization of Multiphase Flow During Impulse Drying," *TAPPI Journal*, Vol. 72, pp. 79-85.